Recent data analysis to revisit the spin structure function of the nucleon in Laplace space

Hoda Nematollahi,[1,*] Abolfazl Mirjalili,[2,†] and Shahin Atashbar Tehrani[3,‡]

[1]*Faculty of Physics, Shahid Bahonar University of Kerman, Kerman, Iran*
[2]*Physics Department, Yazd University, Yazd, Iran*
[3]*School of Particles and Accelerators, Institute for Research in Fundamental Sciences (IPM), P.O.Box 19395-5531, Tehran, Iran*

(Received 10 January 2023; accepted 7 March 2023; published 27 March 2023)

Considering a fixed-flavor number scheme and based on Laplace transformation, we perform leading-order and next-to-leading-order QCD analyses that include world data on polarized structure functions g_1 and g_2. During our analysis, taking the DGLAP evolution equations, we employ the Jacobi polynomials expansion technique. In our recent analysis we utilize the recent available data and consequently include more data than what we did in our previous analysis. We obtain good agreements between our results for the polarized parton densities and nucleon structure functions with all available experimental data and some common parametrization models.

DOI: 10.1103/PhysRevD.107.054033

I. INTRODUCTION

High-energy scattering of polarized leptons by polarized protons, neutrons, and deuterons provides a measurement of the nucleon spin structure functions. These structure functions give information on the polarized quark contributions to the spin of the proton and the neutron and allow tests of the quark-parton model and quantum chromodynamics (QCD). After precise consideration of the unpolarized deep inelastic scattering (DIS) experiments, the polarized DIS program has been planed to study the spin structure of the nucleon using polarized lepton beams (electrons and muons) scattered by polarized targets. These fixed-target experiments have been used to characterize the spin structure of the proton and neutron and also to test fundamental sum rules of QCD and quark-parton model (QPM) [1,2]. The first experiments in polarized electron-polarized proton scattering, performed around 50 years ago, helped to establish the parton structure of the proton. About two decades later, by performing an experiment with a polarized muon and a polarized proton, it has been revealed that the QPM sum rule was violated, which seems to indicate that the quarks do not contribute alone to the spin of the proton. This "proton-spin crisis" gave birth to a new generation of experiments at several high-energy physics laboratories around the world. The new and extensive data sample, collected from these fixed target experiments, has enabled a careful characterization of the spin-dependent parton substructure of the nucleon. The results have been used to test QCD to find an independent value for $\alpha_s(Q^2)$, to probe the polarized parton distributions with reasonable precision, and to provide a first look at the polarized gluon distribution [3].

For this purpose we try to solve the Dokshitzer-Gribov-Lipatov-Altarelli-Parisi (DGLAP) evolution equations using the Laplace transformation. This is done at leading order (LO) and next-to-leading order (NLO) approximations in Secs. II A and II B. We then construct the xg_1 polarized structure function using the expansion in terms of Jacobi polynomials in Sec. III. The evolution of partons requires some inputs that are in fact the polarized parton distribution functions (PPDFs) at an initial energy scale, Q_0^2. On this base we have some parametrizations for the input PPDFs that are introduced in Sec. IV. To determine the unknown parameters of the input PPDFs, we should take all the recent and available data from different DIS experiments. We then use them in a fitting process as is illustrated in Sec. V. Getting the g_1 structure function, it is possible to calculate the g_2 structure function, which is also done in this section. To validate the results from data analysis for the g_1 structure function, several sum rules are computed. We find them in good agreement with experimental data and the results from theoretical investigations in Sec. VI. We employ the last reported data for polarized

*hnematollahi@uk.ac.ir
†Corresponding author.
A.Mirjalili@yazd.ac.ir
‡Atashbar@ipm.ir

targets in DIS experiments. In Sec. VII, we present the compatible results with data at different energy scales, and some models confirm the authenticity of the utilized theoretical framework, including QPM and some outputs of QCD.

II. POLARIZED DGLAP EVOLUTION EQUATIONS IN LAPLACE SPACE

A. Leading-order approximation

In this work we generalize the method of Laplace transformation to employ QCD evolution equations in the polarized case to investigate the polarized parton distributions of the nucleon. Here we focus on the polarization of singlet and nonsinglet quarks to indicate the efficiency of this method for solving the DGLAP evolution equations [4–7]. In order to extract the polarized parton distribution functions, we review the method in this section briefly.

By introducing the variable $\nu \equiv \ln(\frac{1}{x})$ into leading order coupled DGLAP equations, it is possible to turn them into coupled convolution equations in ν space. One can use two Laplace transformations, one from ν space to s space and the second one from τ space to U space, using new the variable $\tau \equiv \frac{1}{4\pi}\int_{Q_0^2}^{Q^2} \alpha_s(Q'^2) d \ln Q'^2$. The DGLAP evolution equations can be solved using these two Laplace transformations and set of convolution integrals of polarized parton distributions at the initial scale Q_0^2. Finally by applying two inverse Laplace transforms, we can return to ordinary space (x, Q^2) [8].

The DGLAP evolution equations for the polarized parton distributions are written as [4–7,9]

$$\frac{4\pi}{\alpha_s(Q^2)}\frac{\partial \Delta F_{NS}}{\partial \ln Q^2}(x,Q^2) = \Delta F_{NS} \otimes \Delta P^0_{qq}(x,Q^2), \quad (1)$$

$$\frac{4\pi}{\alpha_s(Q^2)}\frac{\partial \Delta F_{S}}{\partial \ln Q^2}(x,Q^2) = \Delta F_{S} \otimes \Delta P^0_{qq} + \Delta G \otimes \Delta P^0_{qg}(x,Q^2), \quad (2)$$

$$\frac{4\pi}{\alpha_s(Q^2)}\frac{\partial \Delta G}{\partial \ln Q^2}(x,Q^2) = \Delta F_{S} \otimes \Delta P^0_{gq} + \Delta G \otimes \Delta P^0_{gg}(x,Q^2), \quad (3)$$

where ΔP^0_{ij} s are the LO polarized splitting functions.

By introducing the variable change $w \equiv \ln(1/z)$ and applying two other ones, $v \equiv \ln(1/x)$ and $\tau(Q_0^2, Q^2) \equiv \frac{1}{4\pi}\int_{Q_0^2}^{Q^2} \alpha_s(Q'^2) d \ln Q'^2$, introduced before, and using the notation $\Delta \hat{F}_{NS}(\nu,\tau) \equiv \Delta F_{NS}(e^{-v}, Q^2)$, $\Delta \hat{F}_{NS}(w,\tau) \equiv \Delta F_{NS}(e^{-w},\tau)$, $\Delta \hat{F}_s(\nu,\tau) \equiv \Delta F_s(e^{-v},Q^2)$, $\Delta \hat{F}_s(w,\tau) \equiv \Delta F_s(e^{-w},\tau)$, $\Delta \hat{G}(v,\tau) \equiv \Delta G(e^{-v},\tau)$, $\Delta \hat{G}_s(w,\tau) \equiv \Delta G_s(e^{-w},\tau)$, the above DGLAP equations in terms of the convolution integrals are given as

$$\frac{\partial \Delta \hat{F}_{NS}}{\partial \tau}(v,\tau) = \int_0^v \Delta \hat{F}_{NS}(w,\tau)\Delta \hat{H}^0_{qq}(v-w)dw, \quad (4)$$

$$\frac{\partial \Delta \hat{F}_{S}}{\partial \tau}(v,\tau) = \int_0^v \Delta \hat{F}_{s}(w,\tau)\Delta \hat{H}^0_{qq}(v-w)dw + \int_0^v \Delta \hat{G}_{s}(w,\tau)\Delta \hat{H}^0_{qg}(v-w)dw, \quad (5)$$

$$\frac{\partial \Delta \hat{G}}{\partial \tau}(v,\tau) = \int_0^v \Delta \hat{F}_{s}(w,\tau)\Delta \hat{H}^0_{gq}(v-w) + \int_0^v \Delta \hat{G}_{s}(w,\tau)\Delta \hat{H}^0_{gg}(v-w)dw, \quad (6)$$

where

$$\begin{aligned}
\Delta \hat{H}^0_{qq}(v) &\equiv e^{-v}\Delta P^0_{qq}(e^{-v}),\\
\Delta \hat{H}^0_{gq}(v) &\equiv e^{-v}\Delta P^0_{gq}(e^{-v}),\\
\Delta \hat{H}^0_{qg}(v) &\equiv e^{-v}\Delta P^0_{qg}(e^{-v}),\\
\Delta \hat{H}^0_{gg}(v) &\equiv e^{-v}\Delta P^0_{gg}(e^{-v}).
\end{aligned} \quad (7)$$

By considering the following property of Laplace transforms:

$$\mathcal{L}\left[\int_0^v \Delta \hat{F}[w]\Delta \hat{H}[v-w]dw; s\right] = \mathcal{L}\left[\Delta \hat{F}_s[v]; s\right] \times \mathcal{L}\left[\Delta \hat{H}[v]; s\right], \quad (8)$$

the DGLAP equations in Eqs. (4)–(6) can be converted to three coupled ordinary first-order differential equations in terms of the variable τ in the Laplace s space with τ-dependent coefficients as follows:

$$\begin{aligned}
\frac{\partial \Delta f_{NS}}{\partial \tau}(s,\tau) &= \Delta \Phi^{\mathrm{LO}}_{ns}(s)\Delta f(s,\tau),\\
\frac{\partial \Delta f_{s}}{\partial \tau}(s,\tau) &= \Delta \Phi^{\mathrm{LO}}_{f}(s)\Delta f_s(s,\tau) + \Delta \Theta^{\mathrm{LO}}_{f}(s)\Delta g(s,\tau),\\
\frac{\partial \Delta g}{\partial \tau}(s,\tau) &= \Delta \Phi^{\mathrm{LO}}_{g}(s)\Delta g(s,\tau) + \Delta \Theta^{\mathrm{LO}}_{g}(s)\Delta f_s(s,\tau).
\end{aligned} \quad (9)$$

In the above equations, we utilize the following abbreviations:

$$\begin{aligned}
\Delta f_{NS}(s,\tau) &\equiv \mathcal{L}[\Delta \hat{F}_{NS}(v,\tau); s],\\
\Delta f_{s}(s,\tau) &\equiv \mathcal{L}[\Delta \hat{F}_{s}(v,\tau); s],\\
\Delta g(s,\tau) &\equiv \mathcal{L}[\Delta \hat{G}(v,\tau); s].
\end{aligned} \quad (10)$$

Following that we can write:

$$\begin{aligned}
\mathcal{L}\left[\frac{\partial \Delta \hat{F}_{NS}}{\partial w}(w,\tau); s\right] &= s\Delta f_{NS}(s,\tau),\\
\mathcal{L}\left[\frac{\partial \Delta \hat{F}_{s}}{\partial w}(w,\tau); s\right] &= s\Delta f_{s}(s,\tau),\\
\mathcal{L}\left[\frac{\partial \Delta \hat{G}}{\partial w}(w,\tau); s\right] &= s\Delta g(s,\tau).
\end{aligned} \quad (11)$$

On the other hand the LO coefficients $\Delta\Phi^{\rm LO}$ and $\Delta\Theta^{\rm LO}$ in Laplace s space are given by

$$\Delta\Phi_f^{\rm LO} = 4 - \frac{8}{3}\left(\frac{1}{s+1}+\frac{1}{s+2}+2(\psi^{(0)}(s+1)+\gamma_E)\right), \tag{12}$$

$$\Delta\Theta_f^{\rm LO} = T_r\left(\frac{2}{s+2}-\frac{1}{s+1}\right), \tag{13}$$

$$\Delta\Theta_g^{\rm LO} = C_f\left(\frac{2}{s+1}-\frac{1}{2+s}\right), \tag{14}$$

$$\Delta\Phi_g^{\rm LO} = C_a\left(\frac{11}{6}-\frac{f}{9}+\frac{3}{s+1}-\frac{3}{s+2}+\frac{1}{s+3} + \frac{1}{s+4}+\psi^{(0)}(s+1)-\psi^{(0)}.(s+5)\right). \tag{15}$$

In Eqs. (12) and (15), $\psi^{(0)}(x)$ denotes the digamma function and $\gamma_E = 0.5772156$ is Euler's constant. The evolution of DGLAP equations in Laplace space at the LO approximation for singlet sector and gluon part can be written as

$$\begin{aligned}\Delta f_1(s,\tau) &= \Delta k_{ff_1}(s,\tau)f_0(s) + \Delta k_{fg_1}(s,\tau)g_0(s),\\ \Delta g_1(s,\tau) &= \Delta k_{gg_1}(s,\tau)g_0(s) + \Delta k_{gf_1}(s,\tau)f_0(s),\end{aligned} \tag{16}$$

where the Δks in the above equations are given by

$$\begin{aligned}\Delta k_{ff_1}(s,\tau) &\equiv e^{\frac{\tau}{2}(\Delta\Phi_f^{\rm LO}(s)+\Delta\Phi_g^{\rm LO}(s))}\left[\cos h\left(\frac{\tau}{2}R(s)\right)+\frac{2\sin h(\frac{\tau}{2}R(s))}{R(s)}(\Phi_f^{\rm LO}(s)-\Phi_g^{\rm LO}(s))\right],\\ \Delta k_{fg_1}(s,\tau) &\equiv e^{\frac{\tau}{2}(\Delta\Phi_f^{\rm LO}(s)+\Delta\Phi_g^{\rm LO}(s))}\frac{\sin h(\frac{\tau}{2}R(s))}{R(s)}\Delta\Theta_f^{\rm LO}(s),\\ \Delta k_{gg_1}(s,\tau) &\equiv e^{\frac{\tau}{2}(\Delta\Phi_f^{\rm LO}(s)+\Delta\Phi_g^{\rm LO}(s))}\left[\cos h\left(\frac{\tau}{2}R(s)\right)-\frac{2\sin h(\frac{\tau}{2}R(s))}{R(s)}(\Phi_f^{\rm LO}(s)-\Phi_g^{\rm LO}(s))\right],\\ \Delta k_{fg_1}(s,\tau) &\equiv e^{\frac{\tau}{2}(\Delta\Phi_f^{\rm LO}(s)+\Delta\Phi_g^{\rm LO}(s))}\frac{\sin h(\frac{\tau}{2}R(s))}{R(s)}\Delta\Theta_g^{\rm LO}(s).\end{aligned} \tag{17}$$

In Eq. (17), $R(s)$ is defined as

$$R(s) = \sqrt{(\Delta\Phi_f^{\rm LO}(s)-\Delta\Phi_g^{\rm LO}(s))^2 + 4\Delta\Theta_f^{\rm LO}(s)\Delta\Theta_g^{\rm LO}(s)}. \tag{18}$$

For doing the numerical Laplace inversion in v space, one needs the Laplace inverse of the kernels as $K_{FF}(v,\ \tau)\equiv \mathcal{L}^{-1}[\Delta k_{ff}(s,\ \tau);\ v]$, $K_{FG}(v,\ \tau) \equiv \mathcal{L}^{-1}[\Delta k_{fg}(s,\ \tau);\ v]$, $K_{GF}(v,\tau)\equiv\mathcal{L}^{-1}[\Delta k_{gf}(s,\tau);v]$, and $K_{GG}(v,\tau)\equiv\mathcal{L}^{-1}[\Delta k_{gg}(s,\tau);v]$ [8,10,11]. So that we can write the decoupled solutions in (v,Q^2) space, based on the following convolutions:

$$\begin{aligned}\Delta\hat{F}_s(v,Q^2) &\equiv \int_0^v K_{FF}(v-w,\tau(Q^2,Q_0^2))\Delta\hat{F}_{so}(w)dw\\ &\quad+\int_0^v K_{FG}(v-w,\tau(Q^2,Q_0^2))\Delta\hat{G}_{so}(w)dw,\\ \Delta\hat{G}_s(v,Q^2) &\equiv \int_0^v K_{GG}(v-w,\tau(Q^2,Q_0^2))\Delta\hat{G}_{so}(w)dw\\ &\quad+\int_0^v K_{GF}(v-w,\tau(Q^2,Q_0^2))\Delta\hat{F}_{so}(w)dw.\end{aligned} \tag{19}$$

It is obvious that $\Delta\hat{F}_{so}(w)$ and $\Delta\hat{G}_{so}(w)$ are the Laplace inverse of $f_0(s)$ and $g_0(s)$ in Eq. (16). Reminding $w\equiv\ln(1/z)$ and recalling that $v\equiv\ln(1/x)$, we can finally convert the above solutions into the usual Bjorken-x space.

Now for the nonsinglet sector, $\Delta F_{ns}(x,Q^2)$: as before, if we use the variable change $v\equiv\ln(1/x)$ and the variable τ, then the valance part in Eq. (1) can be written as

$$\frac{\partial\Delta\hat{F}_{NS}}{\partial\tau} = \int_0^v \Delta\hat{F}_{NS}(w,\tau)e^{-(v-w)}\Delta P_{qq}^{{\rm LO},ns}(v-w)dw. \tag{20}$$

Employing the Laplace transformation on above equation, we obtain a linear differential equation in terms of τ variable for the $\Delta f_{ns}(s,\tau)$ as the transformed version of $\Delta\hat{F}_{NS}(x,Q^2)$. This differential equation leads to the following solution:

$$\Delta f_{ns}(s,\tau) \equiv e^{\tau\Delta\Phi_{ns}^{\rm LO}}\Delta f_{ns0}(s). \tag{21}$$

Now using the inverse Laplace transform on Eq. (21) we arrive at the following convolution:

$$\Delta\hat{F}_{ns}(v,\tau) = \int_0^v K_{ns}(v-w,\tau)\Delta\hat{F}_{ns0}(w)dw. \tag{22}$$

In this equation we take $\Delta K_{ns}(v,\tau) \equiv \mathcal{L}^{-1}[e^{\tau\Delta\Phi_{ns}^{\rm LO}(s)}; v]$, where $\Delta\hat{F}_{ns0}(w)$ is the inverse Laplace transform of $\Delta f_{ns0}(s)$. Finally by variable change $\nu = \ln(\frac{1}{x})$ the results in (x, Q^2) space is accessible.

More details to extract parton distribution functions at the LO approximation, based on the Laplace transformation, can be found in [8].

B. Next-leading-order approximation

At the NLO approximation for the nonsinglet sector of DGLAP evolution equation, after changing the required variables that have been introduced before, we arrive at

$$\frac{\partial\hat{\Delta}F_{ns}}{\partial\tau}(\nu,\tau) = \int_0^\nu \Delta\hat{F}_{ns}(w,\tau)e^{-(\nu-w)}\left(\Delta P_{qq}^{\rm LO,ns}(\nu-w) + \frac{\alpha_s(\tau)}{4\pi}\Delta P_{qq}^{\rm NLO,ns}(\nu-w)\right)dw, \tag{23}$$

which is in fact the extended version of Eq. (4) for $\hat{\Delta}F_{ns}$.

Taking the above equation to Laplace s space, we obtain a linear differential equation in terms of the τ variable for the transformed $\Delta f_{ns}(s,\tau)$. This equation has the simple solution as

$$\Delta f_{NS}(s,\tau) = e^{\tau\Delta\Phi_{NS}(s)}\Delta f_{NS}^0(s),$$
$$\Delta\Phi_{NS}(s) \equiv \Delta\Phi_{NS}^{\rm LO}(s) + \frac{\tau_2}{\tau}\Delta\Phi_{NS}^{\rm NLO}(s), \tag{24}$$

where

$$\tau_2 \equiv \frac{1}{4\pi}\int_0^\tau \alpha_s(\tau')d\tau' = \frac{1}{(4\pi)^2}\int_{Q_0^2}^{Q^2}\alpha_s^2(Q'^2)d\,\ln\,Q'^2, \tag{25}$$

and

$$\Delta\Phi_{NS}^{\rm LO}(s) \equiv \mathcal{L}[e^{-v}\Delta P_{qq}^{\rm LO,ns}(e^{-\nu}); s],$$
$$\Delta\Phi_{NS}^{\rm NLO}(s) \equiv \mathcal{L}[e^{-\nu}\Delta P_{qq}^{\rm NLO,NS}(e^{-\nu}); s]. \tag{26}$$

It should be noted that at the LO approximation $\Delta\Phi_{NS}(s) = \Delta\Phi_f^{\rm LO}(s)$, where $\Delta\Phi_f^{\rm LO}(s)$ has been given explicitly in Eq. (12). The evaluation of $\Delta\Phi_{NS}^{\rm NLO}(s)$ has been presented in Ref. [12].

We can find any nonsinglet solution, $\Delta F_{NS}(x,Q^2)$, by applying the nonsinglet kernel $K_{ns}(v) \equiv \mathcal{L}^{-1}[e^{\tau\Delta\Phi_{NS}(s)}; v]$, and using the Laplace convolution relation as

$$\Delta\hat{F}_{NS}(v,\tau) = \int_0^v K_{ns}(v-w,\tau)\Delta\hat{F}_{NS}^0(w)dw. \tag{27}$$

Taking the variable change $\nu \equiv \ln(1/x)$, the results are obtained in (x, Q^2) space as before with the difference that the splitting functions in s space include the NLO contributions corresponding to the following expressions:

$$\Delta\Phi_S(s) \equiv \Delta\Phi_S^{\rm LO}(s) + a_0\Delta\Phi_S^{\rm NLO}(s),$$
$$\Delta\Phi_g(s) \equiv \Delta\Phi_g^{\rm LO}(s) + a_0\Delta\Phi_g^{\rm NLO}(s),$$
$$\Delta\Theta_S(s) \equiv \Delta\Theta_S^{\rm LO}(s) + a_0\Delta\Theta_S^{\rm NLO}(s),$$
$$\Delta\Theta_g(s) \equiv \Delta\Theta_g^{\rm LO}(s) + a_0\Delta\Theta_g^{\rm NLO}(s). \tag{28}$$

The analytical expressions for $\Delta\Phi_{NS}^{\rm NLO}(s)$, $\Delta\Phi_S^{\rm NLO}(s)$, $\Delta\Phi_g^{\rm NLO}(s)$, $\Delta\Theta_S^{\rm NLO}(s)$, and $\Delta\Theta_g^{\rm NLO}(s)$ in Laplace transform s space have been presented in Ref. [12].

We indicate the NLO expression for $\frac{\alpha_s(\tau)}{4\pi}$ by $a(\tau)$. We can numerically show that an excellent approximation to $a(\tau) \equiv \frac{\alpha_s(\tau)}{4\pi}$, with a precision of a few parts in 10^4, is given by the expression

$$a(\tau) \approx a_0 + a_1 e^{-b_1\tau}, \tag{29}$$

where the unknown parameters a_1, b_1, and a_0 are found by a least squared fit to $a(\tau)$. It should be pointed that this approximation is inspired by the fact that, at the LO approximation, the expression for $\alpha_{s,\rm LO}(\tau)$ is exactly given by $\alpha_{s,\rm LO}(Q_0^2)e^{-b\tau}$.

Now for the singlet sector and gluon part of Eq. (9) at the NLO approximation, the results of DGLAP evolution equations in Laplace s space could be obtained and are given by

$$\Delta f(s,\tau) = k_{ff}(a_1,b_1,s,\tau)\Delta f_S^0(s) + k_{fg}(a_1,b_1,s,\tau)\Delta g^0(s),$$
$$\Delta g(s,\tau) = k_{gg}(a_1,b_1,s,\tau)\Delta g^0(s) + k_{gf}(a_1,b_1,s,\tau)\Delta f_S^o(s). \tag{30}$$

Here the functions $k_{ij}(a_1,b_1,s,\tau)$ are expressed as a power series in terms of the NLO expansion parameter a_1 whose coefficients are analytic functions with respect to s and τ parameters. These expressions, which are used to extract polarized parton distribution functions at NLO approximation, can be found in Ref. [12]. Finally, recalling that $\nu \equiv \ln(1/x)$, we can convert the above solutions to the (x, Q^2) space. Therefore we should write the NLO decoupled solutions, $\Delta F_s(x,Q^2)$ and $\Delta G(x,Q^2)$, with the knowledge requirement of $\Delta F(x)$ and $\Delta G(x)$ at the initial scale Q_0^2. We also use these analytical solutions for polarized parton distributions in the next sections to extract polarized structure functions of protons, neutrons, and deuterons.

III. THE JACOBI POLYNOMIAL METHOD

We perform a fit in the LO approximation for the polarized parton distributions using Jacobi polynomials [13–16] to reconstruct the x dependent quantities from their Laplace moments. The application of Jacobi polynomials has a number of advantages; especially, it will provide us an opportunity to factorize out the x and Q^2 dependence,

which help us to have an efficient parametrization and to evolve the structure functions.

For example, we can expand the spin structure function $xg_1(x,Q^2)$, as [14]

$$xg_1(x,Q^2) = x^\beta(1-x)^\alpha \sum_{n=0}^{N_{\max}} a_n(Q^2)\Theta_n^{\alpha,\beta}(x) \quad (31)$$

in which $\Theta_n^{\alpha,\beta}(x)$ are Jacobi polynomials of order n, and $N_{\max}$ is the maximum order of the expansion. In this case, the Q^2 dependence of the polarized structure function is contained in the Jacobi moments, $a_n(Q^2)$. On the other hand, we can factor out the essential part of its x dependence into a weight function using the Jacobi polynomials [17].

For computational purpose, the x dependence of the Jacobi polynomials is given by the following expansion [15]:

$$\Theta_n^{\alpha,\beta}(x) = \sum_{j=0}^{n} c_j^{(n)}(\alpha,\beta)x^j, \quad (32)$$

where the $c_j^{(n)}(\alpha,\beta)$ s are combinations of Γ functions. The Jacobi polynomials satisfy an orthogonality condition with the weight function $x^\beta(1-x)^\alpha$ such that

$$\int_0^1 dx x^\beta(1-x)^\alpha \Theta_k^{\alpha,\beta}(x)\Theta_l^{\alpha,\beta}(x) = \Delta_{k,l}. \quad (33)$$

Hence, the polarized structure function $xg_1(x,Q^2)$ could be reconstructed from Eq. (31) by giving the Jacobi moments $a_n(Q^2)$ [12,18–26].

We can obtain the Jacobi moments $a_n(Q^2)$, taking the orthogonality condition on Eq. (31), which finally lead us to

$$a_n(Q^2) = \sum_{j=0}^{n} c_j^{(n)}(\alpha,\beta)\mathcal{L}[xg_1, s=j+1]. \quad (34)$$

In deriving Eq. (34), we utilize the Laplace transform of $xg_1(x,Q^2)$ as follows:

$$\mathcal{L}[xg_1,s] \equiv \int_0^\infty dv e^{-sv} xg_1(x,Q^2). \quad (35)$$

We can now relate the polarized structure function, $xg_1(x,Q^2)$, with its moments in Laplace s space as follows [12,18–26]:

$$xg_1(x,Q^2) = x^\beta(1-x)^\alpha \sum_{n=0}^{N_{\max}} \Theta_n^{\alpha,\beta}(x) \times \sum_{j=0}^{n} c_j^{(n)}(\alpha,\beta)\mathcal{L}[xg_1, s=j+1]. \quad (36)$$

By regarding Eq. (36) for $xg_1(x,Q^2)$, we choose the set $\{N_{\max},\alpha,\beta\}$ to reach optimal convergence of this series throughout the kinematic region constrained by the data. In practice, we find the following numerical values for above parameters: $N_{\max}=9$, $\alpha=3.0$, and $\beta=0.5$ to be sufficient. We should note that in Mellin space when we intend to calculate the first moment for quark distribution or structure function, g_1, we choose $n=1$, but in Laplace s space to get the first moment, we should consider $s=0$ instead.

IV. QCD ANALYSIS AND PARAMETRIZATION OF PPDFs

The required analysis of PPDFs within the QCD content include the following subsections.

A. Parametrization

We consider a proton consisted of massless partons which carry momentum fraction x with helicity distributions $q_\pm(x,Q^2)$ at characteristic scale Q^2. The difference $\Delta q(x,Q^2) = q_+(x,Q^2) - q_-(x,Q^2)$ measures how much the parton of flavor q remembers its parent's proton polarization. In the other words we can say that it represents the probability of finding a polarized parton with fraction x of parent hadron momentum and spin align/antialign to hadron's spin. It measures the net helicity of partons in a longitudinally polarized hadron.

In parametrization process, we consider the following form for the polarized PDFs at the initial scale $Q_0^2 = 1.3\ \mathrm{GeV}^2$:

$$x\Delta q(x,Q_0^2) = \mathcal{N}_q \eta_q x^{a_q}(1-x)^{b_q}(1+c_q x), \quad (37)$$

in which the polarized PDFs are determined by parameters $\{\eta_q, a_q, b_q, c_q\}$, and the generic label $q = \{u_v, d_v, \bar{q}, g\}$ indicates the partonic flavors up-valence, down-valence, sea, and gluon, respectively. $\mathcal{N}_q$ is the normalization constant given by

$$\frac{1}{\mathcal{N}_q} = \left(1 + c_q \frac{a_q}{a_q+b_q+1}\right) B(a_q, b_q+1), \quad (38)$$

and chosen such that η_q in Eq. (37) is the first moments of $\Delta q(x,Q_0^2)$, where $B(a,b)$ is the Euler beta function.

The total up and down quark distributions are a sum of the valence plus sea distributions: $\Delta u = \Delta u_v + \Delta\bar{q}$ and $\Delta d = \Delta d_v + \Delta\bar{q}$. We consider an $SU(3)$ flavor symmetry as $\Delta\bar{q} \equiv \Delta\bar{u} = \Delta\bar{d} = \Delta s = \Delta\bar{s}$. Nevertheless we could allow for an $SU(3)$ symmetry violation term by introducing κ such that $\Delta s = \Delta\bar{s} = \kappa\Delta\bar{q}$. Since the strange quark distribution is poorly constrained, the results would be insensitive to the particular choice of κ.

From Eq. (37), it is obvious that each of four polarized parton densities $q = \{u_v, d_v, \bar{q}, g\}$ contain four parameters $\{\eta_q, a_q, b_q, c_q\}$, which gives a total of 16 parameters that should be determined. We illustrate that some of these

parameters can be eliminated while maintaining sufficient flexibility to obtain a good fit.

B. First moments of Δu_v and Δd_v

The parameters η_{u_v} and η_{d_v} are the first moments of the polarized valence up and down quark densities, denoted by Δu_v and Δd_v. These densities can be related to F and D quantities as the weak matrix elements that are measured in neutron and hyperon β decays. Hence one can write [27]

$$a_3 = \int_0^1 dx \Delta q_3 = \eta_{u_v} - \eta_{d_v} = F + D, \tag{39}$$

$$a_8 = \int_0^1 dx \Delta q_8 = \eta_{u_v} + \eta_{d_v} = 3F - D, \tag{40}$$

where a_3 and a_8 denote the nonsinglet combinations of the first moments of the polarized quark densities corresponding to

$$q_3 = (\Delta u + \Delta \bar{u}) - (\Delta d + \Delta \bar{d}), \tag{41}$$

$$q_8 = (\Delta u + \Delta \bar{u}) + (\Delta d + \Delta \bar{d}) - 2(\Delta s + \Delta \bar{s}). \tag{42}$$

A reanalysis of F and D with updated β-decay constants leads to the following results: $F = 0.464 \pm 0.008$ and $D = 0.806 \pm 0.008$ [27]. With these values we obtain

$$\eta_{u_v} = +0.928 \pm 0.014, \tag{43}$$

$$\eta_{d_v} = -0.342 \pm 0.018. \tag{44}$$

Utilizing the above numerical values of η_{u_v} and η_{d_v} will end to reduce two parameters during the fitting processes.

C. Polarized DGLAP evolution

The polarized DGLAP evolution equations can be solved in the Laplace space using the Jacobi polynomial approach. The Laplace transformation of the parton densities Δq are defined analogous to that of Eq. (35) as

$$\begin{aligned}\mathcal{L}[\Delta q(x = e^{-v}, Q_0^2), s] &\equiv \Delta q(s, Q_0^2) \\ &= \int_0^\infty e^{-sv} \Delta q(x = e^{-v}, Q_0^2) dv \\ &= \mathcal{N}_q \eta_q \left(1 + c_q \frac{s + a_q}{s + a_q + b_q + 1}\right) \\ &\quad \times B(s + a_q, b_q + 1),\end{aligned} \tag{45}$$

where $q = \{u_v, d_v, \bar{q}, g\}$ and B denotes the Euler beta function.

The twist-2 contributions to the spin-dependent structure function $g_1(s, Q^2)$ can be expressed in terms of the polarized parton densities in the Laplace space as

$$\begin{aligned}\mathcal{L}[g_1^p, s] = \frac{1}{2} \sum_q e_q^2 \times \Bigg[&\left(1 + \frac{\tau}{4\pi} \Delta C_q(s)\right) [\Delta q(s, Q^2) \\ &+ \Delta \bar{q}(s, Q^2)] + \frac{2}{3} \frac{\tau}{4\pi} \Delta C_g(s) \Delta g(s, Q^2)\Bigg],\end{aligned} \tag{46}$$

$$\begin{aligned}\mathcal{L}[g_1^n, s] = \mathcal{L}[g_1^p, s] - \frac{1}{6} &(\mathcal{L}[u_v, s] - \mathcal{L}[d_v, s]) \\ &\times \left(1 + \frac{\tau}{4\pi} \Delta C_q(s)\right).\end{aligned} \tag{47}$$

Here, the summation is over u, d, s quark flavors. $\delta q, \delta \bar{q}$, and δg are the polarized quark, antiquark, and gluon distributions, respectively. ΔC_g and ΔC_q denote the spin-dependent Wilson coefficients in Laplace transform s space, respectively, which are written as

$$\begin{aligned}\Delta C_g = \frac{1}{2} \Bigg(&\frac{2}{s+1} - \frac{2}{s+2} + \frac{\psi^{(0)}(s+1) + \gamma_E}{s+1} \\ &- \frac{2(\psi^{(0)}(s+2) + \gamma_E)}{s+2}\Bigg),\end{aligned} \tag{48}$$

$$\begin{aligned}\Delta C_q = &\frac{8}{3(s+1)} + \frac{4}{3(s+2)} + \frac{4(\psi^{(0)}(s+2) + \gamma_E)}{3(s+1)} \\ &+ \frac{4(\psi^{(0)}(s+3) + \gamma_E)}{3(s+2)} + \frac{4\psi^{(1)}(s+1)}{3} \\ &+ \frac{4\psi^{(1)}(s+3)}{3} - \frac{4}{3}\left(\frac{9}{2} + \frac{\pi^2}{3}\right).\end{aligned} \tag{49}$$

Employing the inverse Laplace transform on Eqs. (46), (47), the g_1^p and g_1^n can be obtained in Bjorken x space. Considering the parametrization for PPDFs there are finally nine unknown parameters that should be determined during the fitting processes, taking the available experimental data for polarized structure functions.

In addition to proton and neutron structure functions we can also do the required computations for the deuteron, which is in fact a nucleus consists of one proton and one neutron. The deuteron structure function is given by $xg_i^d = \frac{xg_i^p + xg_i^n}{2} \times (1 - 1.5\omega_D)$; $i = 1, 2$. Here $\omega_D = 0.05 \pm 0.01$ denotes the probability to find the deuteron in a D state [28–30]. The available data for deuteron structure function are also used during the fitting process.

D. The g_2 structure function

Now by accessing to the g_1 structure function, one can calculate g_2 via the Wandzura-Wilczek [31,32] relation as in the following

$$g_2(x, Q^2) = -g_1^p(x, Q^2) + \int_x^1 \frac{dy}{y} g_1^p(y, Q^2). \tag{50}$$

We are now at the position to investigate the fits to spin-dependent structure functions, as we do it in next section, to extract the PPDFs from the available data.

V. FITTING CONTENTS IN QCD ANALYSIS

A. Overview of datasets

In our recent analysis which we call it NMA23 we focus on the polarized DIS data samples. The needed DIS data for all PPDFs are coming from the experiments at electron-proton collider and also in fixed-target situation including proton, neutron, and heavier targets such as deuteron.

Although separating quarks from antiquarks is not possible, nonetheless it is the inclusive DIS data that is included in the fit. Additionally we take into our NMA23 fitting procedure the g_2 structure function. Due to the technical difficulty in operating the needed transversely polarized target, these data have been traditionally neglected before.

The data which we use in our recent analysis are up to date and include more data than we employed in our pervious analysis [12]. In fact we use all available data of g_1^p from E143, HERMES98, SMC, EMC, E155, HERMES06, COMPASS10, COMPASS16, JLAB06, and JLAB17 experiments [33–42], and g_1^n data from HERMES98, E142, E154, HERMES06, Jlab03, Jlab04, and Jlab05 [34,43–48], and finally the data of g_1^d from E143, SMC, HERMES06, E155, COMPASS05, COMPASS06, and COMPASS17 [33,35,38,49–52]. The DIS data for $g_2^{p,n,d}$ from E143, E142, Jlab03, Jlab04, Jlab05, E155, Hermes12, and SMC [33,43,46–48,53–55] are also included. These datasets are listed in Table I. We also present the kinematic coverage, the number of data points for each given target, and the fitted normalization shifts $\mathcal{N}_i$ in this table. Our NMA23 analysis algorithm calculates the Q^2 evolution and extracts the polarized structure function in x space using Jacobi polynomials approach. By corresponding to the fitting programs on the market, we solve the polarized DGLAP evolution equations in the Laplace space.

One of the important quantities used as criteria to indicate the validation of fit processes is the chi-square (χ^2) test, which assesses the goodness of fit between observed values and those expected theoretically. In next subsection we deal with it in more detail.

B. χ^2 minimization

The goodness of fit to the data for a set of p independent parameters is quantified by the $\chi^2_{\rm global}(\mathrm{p})$. To determine the best fit, we need to minimize the $\chi^2_{\rm global}$ function with the free unknown parameters. We perform it for PPDFs at the LO and NLO approximations that additionally include the QCD cutoff parameter, $\Lambda_{\rm QCD}$, which finally yield us the polarized PDFs at $Q_0^2 = 1.3\ \mathrm{GeV}^2$.

This function is presented as follows:

$$\chi^2_{\rm global}(\mathrm{p}) = \sum_{n=1}^{N_{\rm exp}} w_n \chi^2_n. \tag{51}$$

In above equation, w_n denotes a weight factor for the nth experiment. However this factor in principle can have different values for various datasets, but since all of the experimental datasets have identical worthiness, we take all the related weight factors equal to 1 in our analyses [56–58]. Following that, the χ^2_n in Eq. (51) is defined as

$$\chi^2_n(\mathrm{p}) = \left(\frac{1-\mathcal{N}_{\rm n}}{\Delta\mathcal{N}_{\rm n}}\right)^2 + \sum_{\rm i=1}^{\rm N_n^{data}} \left(\frac{\mathcal{N}_{\rm n} g^{\rm Exp}_{\rm (1,2),i} - g^{\rm Theory}_{\rm (1,2),i}(\mathrm{p})}{\mathcal{N}_{\rm n}\Delta g^{\rm Exp}_{\rm (1,2),i}}\right)^2 \tag{52}$$

The minimization of the $\chi^2_{\rm global}(\mathrm{p})$ function is done applying the CERN program library MINUIT [59]. In the above equation, the essential contribution originates from the difference between the model and the DIS data within the statistical precision. In the χ^2_n function, $g^{\rm Theory}$ indicates the theoretical value for the ith data point and $g^{\rm Exp}$, $\Delta g^{\rm Exp}$ denote the experimental measurement and the experimental uncertainty, respectively, that is coming from statistical and systematic uncertainties, combined in quadrature.

To do a proper fit, we need an overnormalization factor for the data of experiment n that is denoted by $\mathcal{N}_n$. An uncertainty $\Delta\mathcal{N}_n$ is attributed to this factor that should be regarded in the fit. These factors, considering the uncertainties, quoted by the experiments are used to relate different experimental datasets. They are taken as free parameters determined simultaneously with the other parameters in the fit process. In fact they are obtained in the prefitting procedure and then fixed at their best values in further steps. Numerical results of the unknown parameters, obtained from χ^2 minimization, are listed in Table II. Different datasets, used in the fit process, are presented in Table I.

We should remind the reader that the results of fitting process for PPDFs at initial Q_0^2 energy scale is based on Hessian approach [56], such that $\Delta\chi^2/\chi^2 = 0.2\%$, which is corresponding to bigger confidence level (CL) than the inconvenience choice $\Delta\chi^2 = 1$ with 68% CL [60]. The plots for polarized parton densities are depicted in Figs. 1 and 2.

1. Gluon and sea quarks

We find the factor $(1 + c_q x)$ in Eq. (37) provides the flexibility to obtain a good description of the data, especially for the polarized valence quark distributions $\Delta u_v, \Delta d_v$. Thus we will make use of the c_q coefficients for

TABLE I. Summary of published polarized DIS experimental data points with measured x and Q^2 ranges and the number of data points.

Experiment	Reference	$[x_{\min}, x_{\max}]$	$Q^2(\mathrm{GeV}^2)$	Data points	χ^2_{LO}	χ^2_{NLO}	$\mathcal{N}_i$
SLAC/E143(p)	[33]	[0.031–0.749]	1.27–9.52	28	25.9418	25.5862	0.997894385554395
HERMES(p)	[34]	[0.028–0.66]	1.01–7.36	39	57.6213	54.4579	1.00121847577922
SMC(p)	[38]	[0.005–0.480]	1.30–58.0	12	5.7338	7.807	0.999682542198503
EMC(p)	[36]	[0.015–0.466]	3.50–29.5	10	5.5308	5.2507	0.998746870048074
SLAC/E155	[37]	[0.015–0.750]	1.22–34.72	24	30.8939	25.8174	1.00866491330750
HERMES06(p)	[35]	[0.026–0.731]	1.12–14.29	51	25.1976	30.7736	0.978727363512146
COMPASS10(p)	[39]	[0.005–0.568]	1.10–62.10	15	21.1180	21.7614	0.986930436542322
COMPASS16(p)	[40]	[0.0035–0.575]	1.03–96.1	54	38.1731	36.7525	0.998144618082626
SLAC/E143(p)	[33]	[0.031–0.749]	2–3–5	84	108.5918	102.0200	0.998508244589941
HERMES(p)	[34]	[0.023–0.66]	2.5	20	34.3329	32.2223	1.00223612389713
SMC(p)	[38]	[0.003–0.4]	10	12	10.2414	10.2829	1.00050424220605
Jlab06(p)	[41]	[0.3771–0.9086]	3.48–4.96	70	101.8636	103.0134	0.999973926530214
Jlab17(p)	[42]	[0.37696–0.94585]	3.01503–5.75676	82	178.2875	186.4491	1.00223612389713
g_1^p				**501**			
SLAC/E143(d)	[33]	[0.031–0.749]	1.27–9.52	28	37.8573	38.4526	1.00123946481403
SLAC/E155(d)	[49]	[0.015–0.750]	1.22–34.79	24	19.6385	18.3428	1.00093216947938
SMC(d)	[38]	[0.005–0.479]	1.30–54.80	12	19.1969	18.8501	1.00004243740921
HERMES06(d)	[35]	[0.026–0.731]	1.12–14.29	51	48.9197	48.3606	1.00287123838967
COMPASS05(d)	[50]	[0.0051–0.4740]	1.18–47.5	11	8.0128	8.6001	1.00103525695298
COMPASS06(d)	[51]	[0.0046–0.566]	1.10–55.3	15	5.4623	7.6560	1.00014044224998
COMPASS17(d)	[52]	[0.0045–0.569]	1.03–74.1	43	33.1002	31.4721	1.00401646687751
SLAC/E143(d)	[33]	[0.031–0.749]	2–3–5	84	125.8333	125.7379	0.999955538651217
g_1^d				**268**			
SLAC/E142(n)	[43]	[0.035–0.466]	1.10–5.50	8	7.9561	7.7586	0.998697021286838
HERMES(n)	[34]	[0.033–0.464]	1.22–5.25	9	2.3999	2.5486	0.999948762872958
E154(n)	[45]	[0.017–0.564]	1.20–15.00	17	24.3141	21.4152	0.999115473491324
HERMES06(n)	[44]	[0.026–0.731]	1.12–14.29	51	18.2773	17.3811	0.998906625804611
Jlab03(n)	[46]	[0.14–0.22]	1.09–1.46	4	5.6144e − 2	5.7129e − 2	0.999554786214114
Jlab04(n)	[47]	[0.33–0.60]	2.71–4.8	3	14.5393	8.8133	0.994389736514520
Jlab05(n)	[48]	[0.19–0.20]	1.13–1.34	2	7.7029	6.7595	0.999939246942750
g_1^n				**94**			
E143(p)	[33]	[0.038–0.595]	1.49–8.85	12	11.1698	10.9170	1.00335621969896
E155(p)	[53]	[0.038–0.780]	1.1–8.4	8	12.8132	15.6826	1.04042312148245
Hermes12(p)	[54]	[0.039–0.678]	1.09–10.35	20	25.1271	21.5690	1.00274614220085
SMC(p)	[55]	[0.010–0.378]	1.36–17.07	6	1.8259	1.7117	1.00001538561406
g_2^p				**46**			
E143(d)	[33]	[0.038–0.595]	1.49–8.86	12	9.6009	9.6132	1.00047527921467
E155(d)	[53]	[0.038–0.780]	1.1–8.2	8	12.2433	12.275	1.01388492611179
g_2^d				**20**			
E143(n)	[33]	[0.038–0.595]	1.49–8.86	12	8.9660	9.0283	1.00004452228917
E155(n)	[53]	[0.038–0.780]	1.1–8.8	8	14.1622	13.6977	1.03135886789238
E142(n)	[43]	[0.036–0.466]	1.1–5.5	8	16.48220	3.8883	1.00000431789744
Jlab03(n)	[46]	[0.14–0.22]	1.09–1.46	4	17.6171	13.8173	1.03226263480608
Jlab04(n)	[47]	[0.33–0.60]	2.71–4.83	3	4.2782	4.4079	0.900030714490705
Jlab05(n)	[48]	[0.19–0.20]	1.13–1.34	2	10.1400	8.0260	0.981366577296903
g_2^n				**37**			
Total				**966**	**1171.6502**	**1128.9857**	

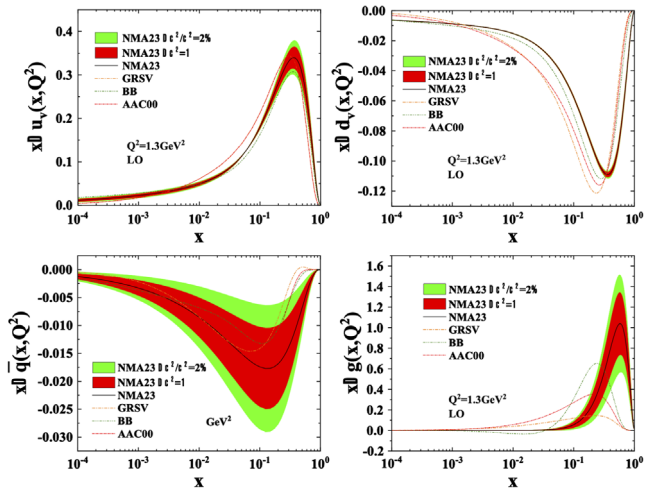

FIG. 1. Our NMA23 results for the polarized PDFs at $Q_0^2 = 1.3$ GeV^2 with respect to x in LO approximation, which is plotted by a solid curve along with their $\Delta\chi^2/\chi^2 = 2\%$ uncertainty bands computed with the Hessian approach. We also present the result obtained in earlier global analyses of BB (dashed) [61], GRSV (dashed dotted) [62], and AAC00 (dashed, dashed, dotted) [63] in LO approximation.

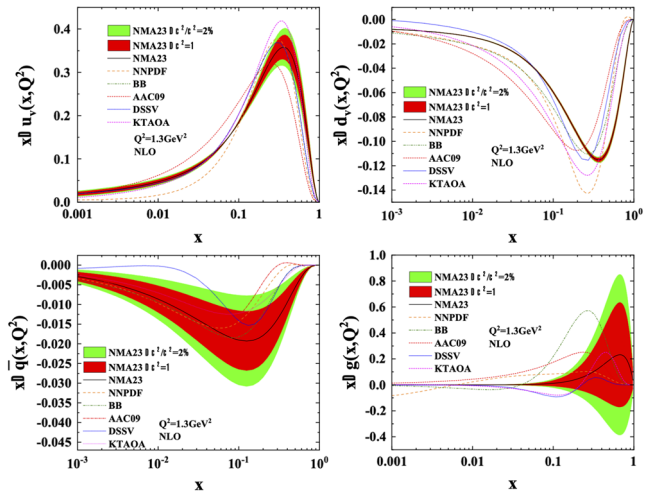

FIG. 2. Our NMA23 results for the spin-dependent PDFs at $Q_0^2 = 1.3$ GeV^2 with respect to x in NLO approximation which is plotted by a solid curve along with their $\Delta\chi^2/\chi^2 = 2\%$ uncertainty bands computed with the Hessian approach. We also display the result obtained in earlier global analyses of NNPDF (dashed, dotted, dotted) [64], KATAO (long dashed) [21], BB (dashed) [65], DSSV (dashed dotted) [66], AAC09 (dashed, dashed, dotted) [67] in NLO approximation.

the up-valence and down-valence quark distribution functions; in contrast, we are able to set the values of $c_{\bar{q}}$ and c_g to zero $(c_{\bar{q}} = c_g = 0)$ while preserving a good fit and eliminating two free parameters. We find that the fit improves if we use nonzero values for the c_{u_v}, c_{d_v} parameters, but as these are relatively flat directions in χ space we shall fix the values as detailed in Table II.

Having fixed η_{u_v}, η_{d_v} and $b_{\bar{q}}, b_g$ parameters in preliminary minimization and taking $c_{\bar{q}} = c_g = 0$, which we referred to before, we then set the $b_{\bar{q}}, b_g, c_{u_v}, c_{d_v}$ parameters as indicated in Table II; this gives us a total of nine unknown parameters, in addition to $\alpha_s(Q_0^2)$.

Now in order to validate the results of the fitting, we consider and calculate some sum rules as we do it in next section.

VI. THE SUM RULES

Some fundamental properties of the nucleon structure can be inspected by considering QCD sum rules like the total momentum fraction carried by partons and also the total contribution of parton spin to the spin of the nucleon. In what follows, by utilizing available experimental data, we analyze some important polarized sum rules.

A. Bjorken sum rule

Integral over the spin distributions of quarks inside the nucleon yields to the polarized Bjorken sum. It can be written in terms of multiplication of nucleon axial charge, g_A (as measured in neutron β decay) with a coefficient function, $C_{Bj}[\alpha_s(Q^2)]$. Taking into account the corrections of higher twist (HT), this sum rule is given by [68]

$$\begin{aligned}\Gamma_1^{\mathrm{NS}}(Q^2) &= \Gamma_1^p(Q^2) - \Gamma_1^n(Q^2),\\ &= \int_0^1 [g_1^p(x,Q^2) - g_1^n(x,Q^2)]dx,\\ &= \frac{1}{6}|g_A|C_{Bj}[\alpha_s(Q^2)] + \text{HT corrections}. \quad (53)\end{aligned}$$

A very precise determination on the α_s as strong coupling constant can be provided by Bjorken sum rule. Using $C_{Bj}[\alpha_s(Q^2)]$ expression the value of coupling can be extracted from experimental data while the present world average value is $\alpha_s(M_Z^2) = 0.1179 \pm 8.5 \times 10^{-6}$ [69]. At four-loop corrections of perturbative QCD this function has been calculated in both massless [70] and massive cases [71]. Due to ambiguities from small-x extrapolation, determining α_s from the Bjorken sum rule is suffering [72]. Nevertheless in our computations the numerical value for coupling constant at Z-boson mass scale can be found during the fitting process to find the unknown parameters of polarized parton densities at initial energy scale Q_0. Outputted results for the coupling constant at LO and NLO analysis are presented in Table II and are in good agreement with the reported world average value of this quantity.

In Table III we list our results for the Bjorken sum rule. Experimental measurements such as E143 [33], SMC [55], HERMES06 [35], and COMPASS16 [40] are added

TABLE II. Final parameter values and their statistical errors in the $\overline{\text{MS}}$ scheme at the input scale $Q_0^2 = 1.3$ GeV^2.

		LO			
Δu_v	η_{u_v}	0.928(Fixed)	$\Delta\bar{q}$	$\eta_{\bar{q}}$	-0.076068 ± 0.0017283
	a_{u_v}	0.2906 ± 0.01061		$a_{\bar{q}}$	0.42486 ± 0.03115
	b_{u_v}	2.0498 ± 0.010617		$b_{\bar{q}}$	2.7562(Fixed)
	c_{u_v}	16.4977(Fixed)		$c_{\bar{q}}$	0
Δd_v	η_{d_v}	−0.342(Fixed)	Δg	η_g	1.1543 ± 0.1792
	a_{d_v}	0.1274 ± 0.003728		a_g	2.4164 ± 0.3716
	b_{d_v}	1.8621 ± 0.044186		b_g	1.7430(Fixed)
	c_{d_v}	35.7909(Fixed)		c_g	0
		$\Lambda = 0.2007 \pm 0.05004$ GeV			
		$\alpha(M_z^2) = 0.12812 \pm 0.0038$			
		$\chi^2/\text{D.O.F.} = 1171.65/957 = 1.224$			
		NLO			
Δu_v	η_{u_v}	0.928(Fixed)	$\Delta\bar{q}$	$\eta_{\bar{q}}$	-0.076272 ± 0.001742
	a_{u_v}	0.33889 ± 0.01121		$a_{\bar{q}}$	0.4844 ± 0.029784
	b_{u_v}	2.1075 ± 0.052585		$b_{\bar{q}}$	3.3948(Fixed)
	c_{u_v}	15.3475(Fixed)		$c_{\bar{q}}$	0
Δd_v	η_{d_v}	−0.342(Fixed)	Δg	η_g	0.2526 ± 0.05528
	a_{d_v}	0.1294 ± 0.004110		a_g	2.0898 ± 0.4409
	b_{d_v}	1.8654 ± 0.043007		b_g	1.0174(Fixed)
	c_{d_v}	41.9067(Fixed)		c_g	0
		$a_1 = 0.0250$ (Fixed)			
		$b_1 = 10.70$ (Fixed)			
		$a_0 = 0.2399$ (Fixed)			
		$\Lambda = 0.2156 \pm 0.04989$ GeV			
		$\alpha(M_z^2) = 0.115457 \pm 0.00341$			
		$\chi^2/\text{D.O.F} = 1128.98/957 = 1.179$			

TABLE III. Our computed LO and NLO results for the Bjorken sum rule, Γ_1^{NS}, in comparison with world data from E143 [33], SMC [55], HERMES06 [35], and COMPASS16 [40]. Only HERMES06 [35] results are not extrapolated in full x range (measured in region $0.021 \leq x \leq 0.9$).

	E143 [33]	SMC [55]	HERMES06 [35]	COMPASS16 [40]	LO	NLO
	$Q^2 = 5$ GeV^2	$Q^2 = 5$ GeV^2	$Q^2 = 5$ GeV^2	$Q^2 = 3$ GeV^2	$Q^2 = 5$ GeV^2	$Q^2 = 5$ GeV^2
Γ_1^{NS}	0.164 ± 0.021	0.181 ± 0.035	0.148 ± 0.017	0.181 ± 0.008	0.15632 ± 0.0062	0.15350 ± 0.00081

to this table. An adequate consistency can be seen between them.

B. Proton helicity sum rule

In order to complete our knowledge in the field of nuclear physics an extrapolation of proton spin among its constituents can be done and consequently new sum rule as proton helicity sum rule is achieved [73]. Considering this sum rule, by a precise extraction of PPDFs, one can obtain an accurate picture of the quark and gluon helicity densities.

Since each constituent of a nucleon is carrying part of nucleon spin, the total spin of nucleon can be written as

$$\frac{1}{2} = \frac{1}{2}\Delta\Sigma(Q^2) + \Delta\text{G}(Q^2) + \text{L}(Q^2). \tag{54}$$

In this equation $\Delta\Sigma(Q^2) = \sum_i \int_0^1 dx(\Delta q(x,Q^2) + \Delta\bar{q}(x,Q^2))$ represents the spin contribution of the singlet flavor, $\Delta\text{G}(Q^2) = \int_0^1 dx\Delta g(x,Q^2)$ denotes the gluon spin contribution, and finally $\text{L}(Q^2)$ is interpreted as the total contribution from quark and gluon orbital angular momentum. In Eq. (54) each term depends on Q^2, but the sum of them does not. The measuring processes of them cannot be done easily and it is beyond the scope of this paper to describe their measurement methods.

TABLE IV. Results for the full and truncated first moments of the polarized singlet-quark $\Delta\Sigma(Q^2) = \sum_i \int_0^1 dx[\Delta q_i(x) + \Delta\bar{q}_i(x)]$ and gluon distributions at the scale $Q^2 = 10$ GeV^2 in the $\overline{\text{MS}}$ scheme. The recent polarized global analysis of NNPDFpol1.1 [74] and DSSV14 [66] are also presented.

	DSSV14 [66]	NNPDFpol1.1 [74]	LO	NLO
Full x region [0, 1]				
$\Delta\Sigma(Q^2)$	0.291799	$+0.18 \pm 0.21$	0.12959 ± 0.00922	0.148546 ± 0.0194
$\Delta G(Q^2)$	0.37109	0.03 ± 3.24	1.4693 ± 1.049	0.8626 ± 0.3054
Truncated x region $[10^{-3}, 1]$				
$\Delta\Sigma(Q^2)$	0.36645	$+0.25 \pm 0.10$	0.03644 ± 0.0406	0.04848 ± 0.0187
$\Delta G(Q^2)$	0.3636	0.49 ± 0.75	1.3848 ± 0.9829	0.7827 ± 0.2854

Numerical values of first moments of the singlet-quark and gluon at $Q^2 = 10$ GeV^2 are listed in Table IV. Our results at both truncated and full x region are compared to those from the NNPDFpol1.1 [74] and DSSV14 [66].

As can be seen from Table IV for $\Delta\Sigma$, our NMA23 results are consistent, within uncertainty, with those of other groups. This occurs because in semileptonic decays the first moment of polarized densities are mainly fixed. Very different values are reported by various groups when the gluon contribution is considered. Due to their large uncertainty we avoid getting a stiff result for the full first moment of gluon.

The proton spin sum rule can be finally calculated considering the extracted values that are listed in Table IV. Accordingly, the numerical value of quark and gluon orbital angular momentum, attributed to the spin of the proton, is obtained as

$$L(Q^2 = 10\ \text{GeV}^2) = -0.436873 \pm 0.334587. \quad (55)$$

The contribution of the total orbital angular momentum to the spin of the proton cannot be determined tightly, and it is due to the large uncertainty that is mostly coming out from the gluons. By improving the current level of experimental accuracy, the precise determination of each individual contribution to the nucleon spin can be obtained.

C. The twist-3 reduced matrix element d_2

Twist-3 reduced matrix element, denoted by d_2, is not considered as a sum rule but to investigate the higher twist effect, the numerical evaluation of this quantity is important. One can find in [65] the detailed analyses of higher twist, related to the g_1 polarized structure function. Through the moments of g_1 and g_2 structure functions, considering the operator product expansion theorem [75], the effect of quark-gluon correlations can be studied. These considerations for the moments will conclude the following definition for $d_2(Q^2)$ as a reduced matrix element:

$$d_2(Q^2) = 3\int_0^1 x^2 \bar{g}_2(x, Q^2)dx, = \int_0^1 x^2[3g_2(x, Q^2) + 2g_1(x, Q^2)]dx. \quad (56)$$

In the above equation we have $\bar{g}_2 = g_2 - g_2^{\text{WW}}$, where g_2^{WW}, corresponding to Eq. (50), is given by Wandzura and Wilczek (WW). The deviation of g_2 from $g_2^{\tau_2}$, which is the polarized structure function at leading twist order can be measured using the $d_2(Q^2)$ as the twist-3 reduced matrix element of spin-dependent operators in nucleon. This matrix element, because of the x^2 weighting factor in Eq. (56), is remarkably sensitive to the behavior of $\bar{g}_2$ at large-x values. By extracting the d_2 term, valuable intuition about the size of the multiparton correlation terms can be achieved that denotes the importance of this quantity.

Having a nonzero value for d_2 reveals the importance of higher twist terms in QCD analyses. To improve model prediction, more information on the higher twist operators are required, and this can be done with a precise measurement of the d_2 term. Our results for d_2, compared with experimental values and also some theoretical predictions, are presented in Table V.

D. Burkhardt-Cottingham sum rule

The zeroth moment of g_2 structure function, considering dispersion relations for virtual Compton scattering at all Q^2 values, is predicted to get zero value, and consequently the Burkhardt and Cottingham (BC) sum rule is obtained [82]:

$$\Gamma_2 = \int_0^1 dx\, g_2(x, Q^2) = 0. \quad (57)$$

The BC sum rule is an insignificant result, arising out from the WW relation that is given by Eq. (50). In light cone expansion, one cannot obtain the zeroth moment of structure function and hence local operator product

TABLE V. d_2 moments of the proton, neutron and deuteron polarized structure functions from the SLAC E155x [53], E01-012 [76], E06-014 [77], lattice QCD [78], CM bag model [79], JAM15 [80], JAM13 [81] compared with LO and NLO results.

	Reference	Q^2 [GeV^2]	$10^2 d_2^p$	$10^5 d_2^n$	$10^3 d_2^d$
LO		5	0.2994 ± 0.00035	127.68 ± 11.0073	1.2534 ± 0.02719
NLO		5	0.2855 ± 0.00196	23.4919 ± 0.6654	1.3464 ± 0.0743
E06-014	[77]	3.21		$-421.0 \pm 79.0 \pm 82.0 \pm 8.0$	⋯
E06-014	[77]	4.32		$-35.0 \pm 83.0 \pm 69.0 \pm 7.0$	⋯
E01-012	[76]	3	⋯	$-117 \pm 88 \pm 138$	⋯
E155x	[53]	5	0.32 ± 0.17	790 ± 480	⋯
E143	[33]	5	0.58 ± 0.50	500 ± 2100	5.1 ± 9.2
Lattice QCD	[78]	5	0.4(5)	$-100(-300)$	⋯
CM bag model	[79]	5	1.74	-253	6.79
JAM15	[80]	1	0.5 ± 0.2	-100 ± 100	⋯
JAM13	[81]	5	1.1 ± 0.2	200 ± 300	⋯

TABLE VI. The result of BC sum rule for Γ_2^p, Γ_2^d and Γ_2^n in comparison with world data from E143 [33], E155 [53], HERMES2012 [54], RSS [85], E01012 [76].

	E143 [33] $0.03 \le x \le 1$ $Q^2 = 5$ GeV^2	E155 [53] $0.02 \le x \le 0.8$ $Q^2 = 5$ GeV^2	HERMES2012 [54] $0.023 \le x \le 0.9$ $Q^2 = 5$ GeV^2	RSS [85] $0.316 < x < 0.823$ $Q^2 = 1.28$ GeV^2	E01012 [76] $0 \le x \le 1$ $Q^2 = 3$ GeV^2	LO $0.03 \le x \le 1$ $Q^2 = 5$ GeV^2	NLO $0.03 \le x \le 1$ $Q^2 = 5$ GeV^2
Γ_2^p	-0.014 ± 0.028	-0.044 ± 0.008	0.006 ± 0.029	-0.0006 ± 0.0022	⋯	-0.01911 ± 0.0199	-0.01929 ± 0.00038
Γ_2^d	-0.034 ± 0.082	-0.008 ± 0.012	⋯	-0.0090 ± 0.0026	⋯	-0.001687 ± 0.000016	-0.0028986 ± 0.00053
Γ_2^n	⋯	⋯	⋯	-0.0092 ± 0.0035	0.00015 ± 0.00113	0.007824 ± 0.00056	0.0034500 ± 0.000016

expansion [83] cannot describe this moment. This sum rule can be used even if the structure function involves target mass correction [84]. Finally it should be said that the presence of the HT contribution is denoting the violation of the BC sum rule [54].

In Table VI we list our results for Γ_2 at LO and NLO approximations where data from E143 [33], E155 [53], HERMES2012 [54], RSS [85], E01012 [76] groups for proton, deuteron, and neutron are also added there. The behavior of the g_2 structure function at low-x values has not yet measured accurately but it has a significant effect on any possible conclusions we get.

VII. CONCLUSION

For about three decades, studies of the internal spin structure of the proton have advanced steadily using the technology of polarized beams and polarized targets. The demand for higher-energy experiments to access the deepest regions inside the proton and to extract the theoretically cleanest results continues.

Polarized deep inelastic scattering remains one of the cleanest tests for studying the internal spin structure of the proton and neutron. Pioneering experiments at SLAC, scattering polarized electrons off polarized protons, helped to establish the quark structure of the proton with the observation of large spin-dependent asymmetries. An exciting follow-up experiment (CERN EMC) at higher energies uncovered a violation of the quark parton model sum rule, implying that the quarks accounted for only a

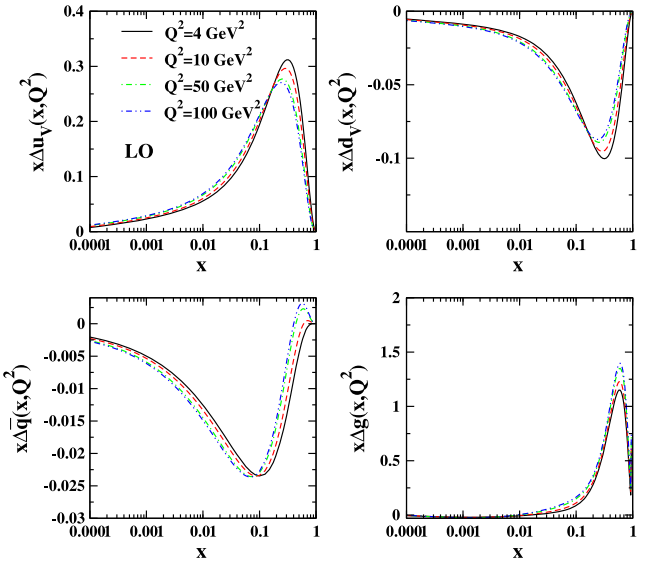

FIG. 3. The evolved polarized quark densities as a function of x in the LO approximation.

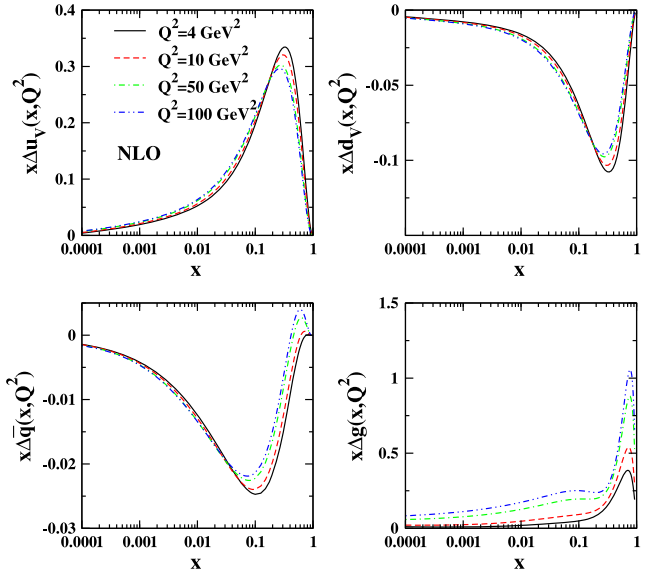

FIG. 4. The evolved polarized quark densities as a function of x in the NLO approximation.

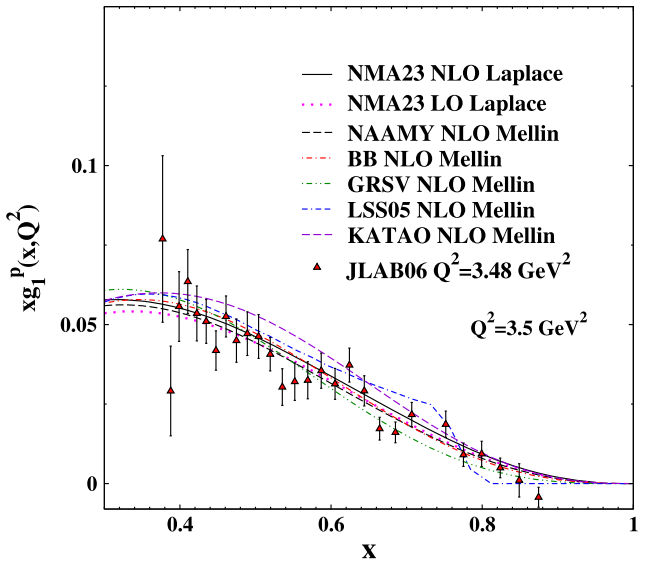

FIG. 6. As in Fig. 5 but at $Q^2 = 3.5$ GeV^2 and in a shorter range of x, corresponding to the available data.

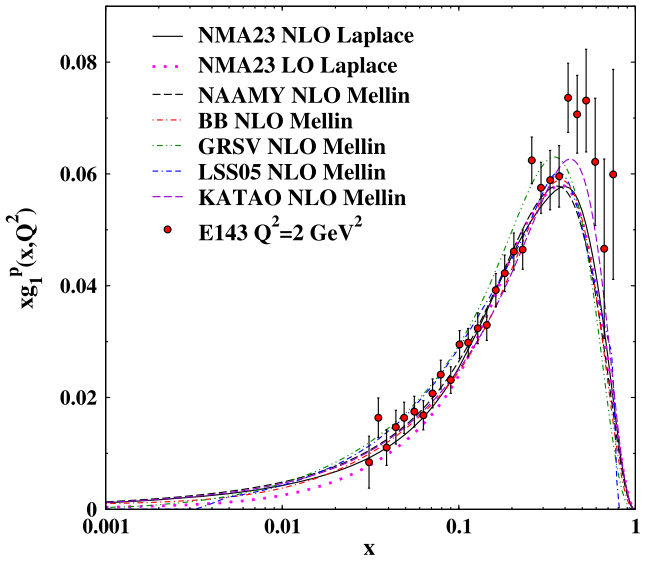

FIG. 5. The polarized proton structure functions with respect to x at $Q^2 = 2$ GeV^2. The results of Jacobi expansion technique in NLO (solid curve) and LO (dotted) approximations are compared with parametrization models such as NAAMY (long dashed) [25], BB (dashed dotted) [65], GRSV (dashed, dotted, dotted) [62], LSS05 (dashed, dashed, dotted) [86], and KATAO (dashed) [21].

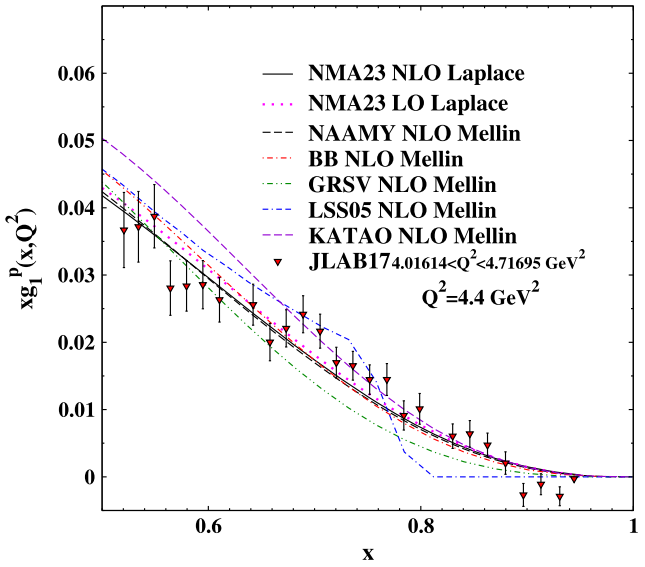

FIG. 7. As in Fig. 5 but at $Q^2 = 4.4$ GeV^2 and in a shorter range of x, corresponding to the available data.

small fraction of the proton spin and giving birth to the proton-spin crisis. Since about three decades ago a large sample of data from polarized fixed-target experiments at SLAC, CERN, and DESY have resulted in a substantial perturbative-QCD analysis of the nucleon spin structure.

Determining the nucleon spin structure functions $g_1(x, Q^2)$ and $g_2(x, Q^2)$ and their moments is the main goal of our present NMA23 analysis. They are essential to test some QCD sum rules. We provided a unified and consistent PPDF through an achievement containing an appropriate description of the fitted data. Within the known very large uncertainties arising from the lack of constraining data, our helicity distributions are in good consistency with other extractions. We studied the Bjorken sum rule, proton helicity, and Burkhardt-Cottinghan sum

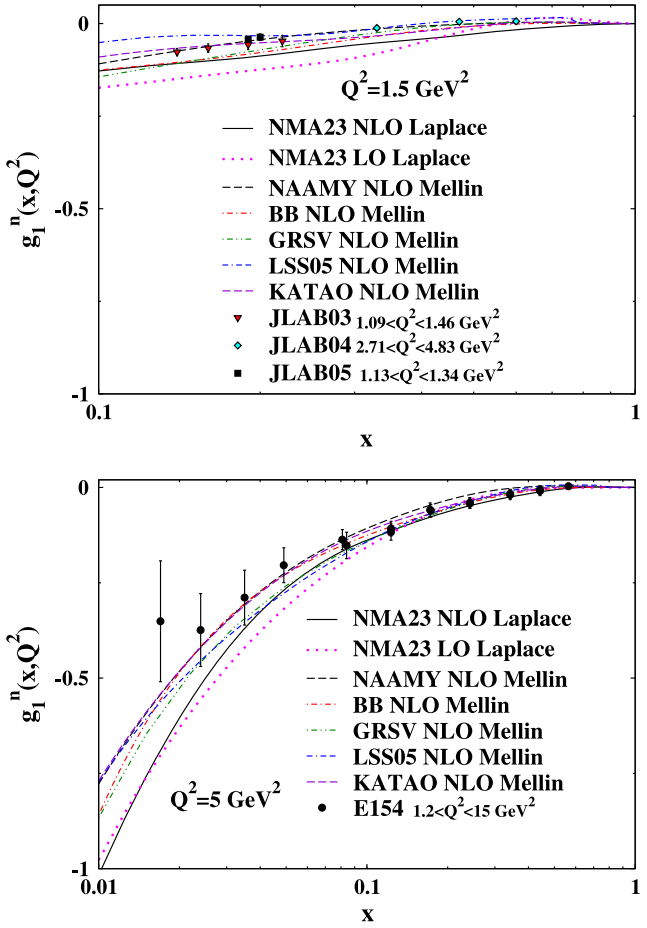

FIG. 8. The spin-dependent neutron structure functions with respect to x at $Q^2 = 1.5$ and 5 GeV^2. The results of Jacobi expansion technique in NLO (solid curve) and LO (dotted) approximations are compared with parametrization models like NAAMY (long dashed) [25], BB (dashed dotted) [65], GRSV (dashed, dotted, dotted) [62], LSS05 (dashed, dashed, dotted) [86], and KATAO (dashed) [21].

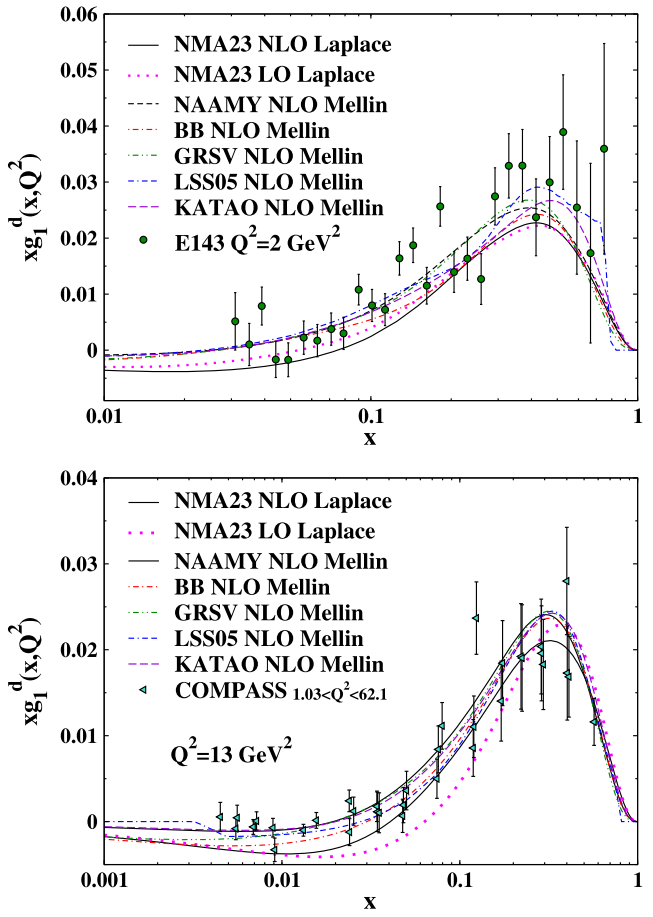

FIG. 9. The spin-dependent structure functions of deuteron as a function of x at $Q^2 = 2$ and 13 GeV^2. The results of Jacobi expansion technique in NLO (solid curve) and LO (dotted) approximations are compared with parametrization models such as NAAMY (long dashed) [25], BB (dashed dotted) [65], GRSV (dashed, dotted, dotted) [62], LSS05 (dashed, dashed, dotted) [86], and KATAO (dashed) [21].

rules. Our results for the reduced matrix element d2 at the NLO approximation have also been presented. To investigate them precisely, more accurate data are needed, and in this work we considered all the recent and available data relating to polarized targets that are listed in Table I.

Using the Jacobi polynomial technique, a fit to the polarized lepton DIS data on nucleon have been presented at the NLO approximation. We found good agreement with the experimental data and our results have correspond with determinations from some parametrization models. In general we could demonstrate that an acceptable progression has been achieved describing the spin structure of the nucleon.

The available data that we use in our recent analysis are up to date and include more data than we employed in our previous analysis [12]. These datasets are summarized in Table I. The kinematic coverage, the number of data points for each given target, and the fitted normalization shifts N_i are also presented in this table. Our NMA23 analysis algorithm computed the Q^2 evolution and extracted the spin structure functions in x space using Jacobi polynomials approach. It corresponded to the fitting programs of other groups that solve the DGLAP evolution equations in the Mellin space. Results for PPDFs at different energy scales and $g_1^{p,n}$ structure functions, together with the deuteron nucleus, have been presented in Figs. 1–11, which confirm the validity of computations during the fitting process to all updated and recent related data.

In the future, the current analysis can be extended to include transverse polarized targets, using the Jacobi polynomial expansions in Laplace s space or other polynomial expansion.

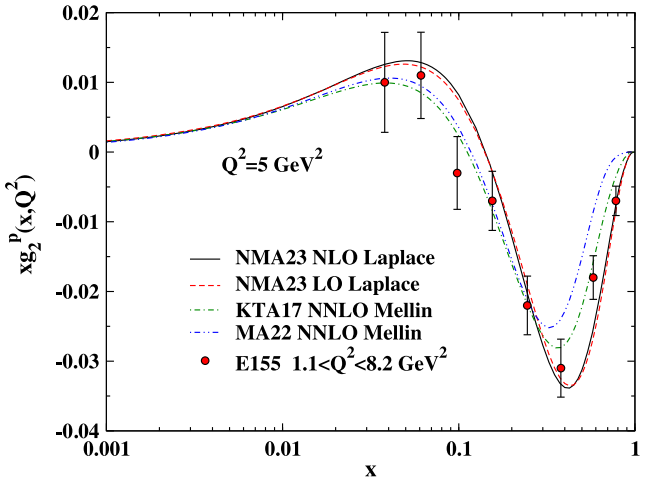

FIG. 10. The polarized proton structure functions xg_2^p as a function of x at $Q^2 = 5$ GeV^2. The results of Jacobi expansion technique in NLO (solid curve) and LO (dashed) approximations are compared with parametrization models like KTA17 (dashed dotted) [19], MA22 (dashed, dotted, dotted) [26].

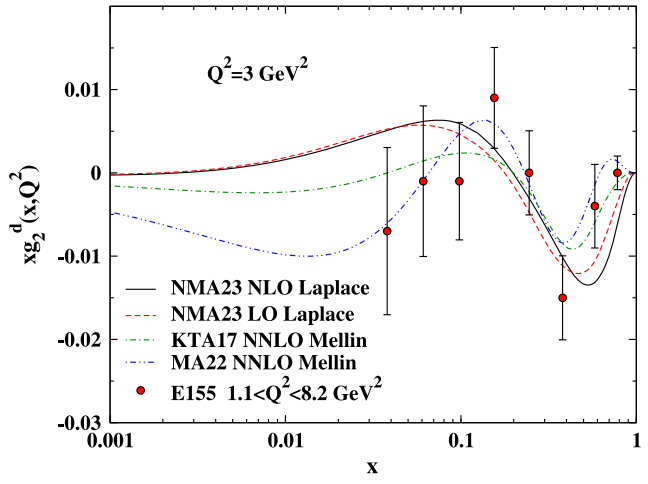

FIG. 11. The spin-dependent deuteron structure functions xg_2^d with respect to x at $Q^2 = 3$ GeV^2. The result of Jacobi expansion technique in NLO (solid curve) and LO (dashed) approximations are compared with parametrization models like KTA17 (dashed dotted) [19], MA22 (dashed, dotted, dotted) [26].

ACKNOWLEDGMENTS

H. N. is indebted to Shaid Bahonar university of Kerman and A. M. acknowledges Yazd University for the provided facilities to do this project. S. A. T. is grateful to the School of Particles and Accelerators, Institute for Research in Fundamental Sciences (IPM) for the required support to do this project.

[1] E. W. Hughes and R. Voss, Annu. Rev. Nucl. Part. Sci. **49**, 303 (1999).
[2] A. Deur, S. J. Brodsky, and G. F. de Téramond, Rep. Prog. Phys. **82**, 076201 (2019).
[3] W. Zhu and J. Ruan, Int. J. Mod. Phys. E **24**, 1550077 (2015).
[4] Y. L. Dokshitzer, Sov. Phys. JETP **46**, 641 (1977) [Zh. Eksp. Teor. Fiz. **73**, 1216 (1977)].
[5] V. N. Gribov and L. N. Lipatov, Sov. J. Nucl. Phys. **15**, 438 (1972) [Yad. Fiz. **15**, 781 (1972)].
[6] L. N. Lipatov, Sov. J. Nucl. Phys. **20**, 94 (1975) [Yad. Fiz. **20**, 181 (1974)].
[7] G. Altarelli and G. Parisi, Nucl. Phys. **B126**, 298 (1977).
[8] M. M. Block, L. Durand, P. Ha, and D. W. McKay, Eur. Phys. J. C **69**, 425 (2010).
[9] W. Furmanski and R. Petronzio, Z. Phys. C **11**, 293 (1982).
[10] M. M. Block, Eur. Phys. J. C **68**, 683 (2010).
[11] M. M. Block, Eur. Phys. J. C **65**, 1 (2010).
[12] S. Atashbar Tehrani, F. Taghavi-Shahri, A. Mirjalili, and M. M. Yazdanpanah, Phys. Rev. D **87**, 114012 (2013); **88**, 039902(E) (2013).
[13] A. L. Kataev, A. V. Kotikov, G. Parente, and A. V. Sidorov, Phys. Lett. B **417**, 374 (1998).
[14] A. L. Kataev, G. Parente, and A. V. Sidorov, Nucl. Phys. **B573**, 405 (2000).
[15] A. L. Kataev, G. Parente, and A. V. Sidorov, Fiz. Elem. Chastits At. Yadra **34**, 43 (2003) [Phys. Part. Nucl. **38**, 827 (2007)].
[16] A. L. Kataev, G. Parente, and A. V. Sidorov, arXiv:hep-ph/9809500.
[17] G. Parisi and N. Sourlas, Nucl. Phys. **B151**, 421 (1979); I. S. Barker, C. S. Langensiepen, and G. Shaw, Nucl. Phys. **B186**, 61 (1981).
[18] F. Taghavi-Shahri, H. Khanpour, S. Atashbar Tehrani, and Z. Alizadeh Yazdi, Phys. Rev. D **93**, 114024 (2016).
[19] H. Khanpour, S. T. Monfared, and S. Atashbar Tehrani, Phys. Rev. D **95**, 074006 (2017).
[20] H. Khanpour, S. T. Monfared, and S. Atashbar Tehrani, Phys. Rev. D **96**, 074037 (2017).
[21] A. N. Khorramian, S. Atashbar Tehrani, S. Taheri Monfared, F. Arbabifar, and F. I. Olness, Phys. Rev. D **83**, 054017 (2011).
[22] A. N. Khorramian, H. Khanpour, and S. A. Tehrani, Phys. Rev. D **81**, 014013 (2010).
[23] S. M. Moosavi Nejad, H. Khanpour, S. Atashbar Tehrani, and M. Mahdavi, Phys. Rev. C **94**, 045201 (2016).
[24] H. Khanpour, A. Mirjalili, and S. Atashbar Tehrani, Phys. Rev. C **95**, 035201 (2017).
[25] H. Nematollahi, P. Abolhadi, S. Atashbar, A. Mirjalili, and M. M. Yazdanpanah, Eur. Phys. J. C **81**, 18 (2021).

[26] A. Mirjalili and S. Tehrani Atashbar, Phys. Rev. D **105**, 074023 (2022).
[27] C. Amsler *et al.* (Particle Data Group), Phys. Lett. B **667**, 1 (2008).
[28] M. Lacombe *et al.*, Phys. Lett. **101B**, 139 (1981).
[29] W. W. Buck and F. Gross, Phys. Rev. D **20**, 2361 (1979).
[30] M. J. Zuilhof and J. A. Tjon, Phys. Rev. C **22**, 2369 (1980).
[31] S. Wandzura and F. Wilczek, Phys. Lett. **72B**, 195 (1977).
[32] A. Piccione and G. Ridolfi, Nucl. Phys. **B513**, 301 (1998).
[33] K. Abe *et al.* (E143 Collaboration), Phys. Rev. D **58**, 112003 (1998).
[34] A. Airapetian *et al.* (HERMES Collaboration), Phys. Lett. B **442**, 484 (1998).
[35] A. Airapetian *et al.* (HERMES Collaboration), Phys. Rev. D **75**, 012007 (2007).
[36] J. Ashman *et al.* (European Muon Collaboration), Phys. Lett. B **206**, 364 (1988).
[37] P. L. Anthony *et al.* (E155 Collaboration), Phys. Lett. B **493**, 19 (2000).
[38] B. Adeva *et al.* (Spin Muon Collaboration), Phys. Rev. D **58**, 112001 (1998).
[39] M. G. Alekseev *et al.* (COMPASS Collaboration), Phys. Lett. B **690**, 466 (2010); V. Y. Alexakhin *et al.* (COMPASS Collaboration), Phys. Lett. B **647**, 8 (2007).
[40] C. Adolph *et al.* (COMPASS Collaboration), Phys. Lett. B **753**, 18 (2016).
[41] K. V. Dharmawardane *et al.* (CLAS Collaboration), Phys. Lett. B **641**, 11 (2006).
[42] R. Fersch *et al.* (CLAS Collaboration), Phys. Rev. C **96**, 065208 (2017).
[43] P. L. Anthony *et al.* (E142 Collaboration), Phys. Rev. D **54**, 6620 (1996).
[44] K. Ackerstaff *et al.* (HERMES Collaboration), Phys. Lett. B **404**, 383 (1997).
[45] K. Abe *et al.* (E154 Collaboration), Phys. Rev. Lett. **79**, 26 (1997).
[46] K. M. Kramer (Jefferson Lab E97-103 Collaboration), AIP Conf. Proc. **675**, 615 (2003).
[47] X. Zheng *et al.* (Jefferson Lab Hall A Collaboration), Phys. Rev. C **70**, 065207 (2004).
[48] K. Kramer *et al.*, Phys. Rev. Lett. **95**, 142002 (2005).
[49] P. L. Anthony *et al.* (E155 Collaboration), Phys. Lett. B **463**, 339 (1999).
[50] E. S. Ageev *et al.* (COMPASS Collaboration), Phys. Lett. B **612**, 154 (2005).
[51] V. Y. Alexakhin *et al.* (COMPASS Collaboration), Phys. Lett. B **647**, 8 (2007).
[52] C. Adolph *et al.* (COMPASS Collaboration), Phys. Lett. B **769**, 34 (2017).
[53] P. L. Anthony *et al.* (E155 Collaboration), Phys. Lett. B **553**, 18 (2003).
[54] A. Airapetian *et al.*, Eur. Phys. J. C **72**, 1921 (2012).
[55] D. Adams *et al.* (Spin Muon Collaboration (SMC)), Phys. Rev. D **56**, 5330 (1997).
[56] J. Pumplin, D. Stump, R. Brock, D. Casey, J. Huston, J. Kalk, H. L. Lai, and W. K. Tung Phys. Rev. D **65**, 014013 (2001).
[57] H. Paukkunen and P. Zurita, J. High Energy Phys. 12 (2014) 100.
[58] C. Han, G. Xie, R. Wang, and X. Chen, Nucl. Phys. **B985**, 116012 (2022).
[59] F. James and M. Roos, Comput. Phys. Commun. **10**, 343 (1975).
[60] D. de Florian, R. Sassot, M. Stratmann, and W. Vogelsang, Phys. Rev. D **80**, 034030 (2009).
[61] J. Blumlein and H. Bottcher, Nucl. Phys. **B636**, 225 (2002).
[62] M. Gluck, E. Reya, M. Stratmann, and W. Vogelsang, Phys. Rev. D **63**, 094005 (2001).
[63] Y. Goto *et al.* (Asymmetry Analysis Collaboration), Phys. Rev. D **62**, 034017 (2000).
[64] E. R. Nocera *et al.* (NNPDF Collaboration), Nucl. Phys. **B887**, 276 (2014).
[65] J. Blumlein and H. Bottcher, Nucl. Phys. **B841**, 205 (2010).
[66] D. de Florian, R. Sassot, M. Stratmann, and W. Vogelsang, Phys. Rev. Lett. **113**, 012001 (2014).
[67] M. Hirai *et al.* (Asymmetry Analysis Collaboration), Nucl. Phys. **B813**, 106 (2009).
[68] J. D. Bjorken, Phys. Rev. D **1**, 1376 (1970).
[69] P. A. Zyla *et al.* (Particle Data Group), Prog. Theor. Exp. Phys. **2020**, 083C01 (2020).
[70] P. A. Baikov, K. G. Chetyrkin, and J. H. Kuhn, Phys. Rev. Lett. **104**, 132004 (2010).
[71] J. Blümlein, G. Falcioni, and A. De Freitas, Nucl. Phys. **B910**, 568 (2016).
[72] G. Altarelli, R. D. Ball, S. Forte, and G. Ridolfi, Acta Phys. Pol. B **29**, 1145 (1998).
[73] E. Leader, arXiv:hep-ph/1604.00305.
[74] E. R. Nocera *et al.* (NNPDF Collaboration), Nucl. Phys. **B887**, 276 (2014).
[75] J. C. Collins, *Renormalization: An Introduction to Renormalization, the Renormalization Group and the Operator-Product Expansion* (Cambridge University Press, Cambridge, England, 1984).
[76] P. Solvignon *et al.* (E01-012 Collaboration), Phys. Rev. C **92**, 015208 (2015).
[77] D. Flay *et al.*, Phys. Rev. D **94**, 052003 (2016).
[78] M. Gockeler *et al.*, Phys. Rev. D **72**, 054507 (2005).
[79] X. Song, Phys. Rev. D **54**, 1955 (1996).
[80] N. Sato, W. Melnitchouk, S. E. Kuhn, J. J. Ethier, and A. Accardi (Jefferson Lab Angular Momentum Collaboration), Phys. Rev. D **93**, 074005 (2016).
[81] P. Jimenez-Delgado, A. Accardi, and W. Melnitchouk, Phys. Rev. D **89**, 034025 (2014).
[82] H. Burkhardt and W. N. Cottingham, Ann. Phys. (N.Y.) **56**, 453 (1970).
[83] J. Blumlein and N. Kochelev, Nucl. Phys. **B498**, 285 (1997).
[84] J. Blumlein and A. Tkabladze, Nucl. Phys. **B553**, 427 (1999).
[85] K. Slifer *et al.* (Resonance Spin Structure Collaboration), Phys. Rev. Lett. **105**, 101601 (2010).
[86] E. Leader, A. V. Sidorov, and D. B. Stamenov, Phys. Rev. D **73**, 034023 (2006).